JOURNAL OF MECHANICS OF CONTINUA AND MATHEMATICAL SCIENCES
www.journalimcms.org

ISSN (Online) : 2454 -7190 Vol.-21, No.-05, May (2026) pp 41-59 ISSN (Print) 0973-8975

DESIGN AND OPTIMIZATION OF A HIGH-EFFICIENCY CRESCENT-SHAPED MICROSTRIP ANTENNA FOR MULTIBAND WIRELESS AND RF ENERGY HARVESTING SYSTEMS

Hawraa Hussain Jabor Zamil[1], Haider TH. Salim ALRikabi[2]

[1,2] Electrical Engineering Department, College of Engineering, Wasit University, Wasit, ALKut, Iraq.

Email: [1]Std2024203.h.h@uowasit.edu.iq, [2]hdhiyab@uowasit.edu.iq

Corresponding Author: **Haider TH. Salim ALRikabi**

https://doi.org/10.26782/jmcms.2026.05.00004

(Received: February 20, 2026; Revised: April 19, 2026; Accepted : May 02, 2026)

Abstract

This paper presents the design, simulation, fabrication, and experimental validation of an etched crescent-shaped microstrip patch antenna for compact multiband wireless communication and radio frequency energy harvesting (RFEH) applications. Through a systematic design evolution process, six antenna configurations are investigated. Two of these were fabricated. ***Design 5 represents the optimum configuration and exhibits the best overall electromagnetic performance among all investigated designs.*** *It achieves excellent impedance matching with a minimum fabricated reflection coefficient of (-31 dB, -20dB, and -30dB) at (1.9, 4.2, and 5.2) GHz, respectively, and VSWR close to 1. This design demonstrates a peak gain of approximately 5.1 dBi and very high radiation and total efficiencies exceeding 93%, indicating efficient power transfer and low loss despite the use of an FR-4 substrate with dimensions of 60 × 40 × 1.6 mm³, employing a partial ground plane and a 50-Ω microstrip feed line. The final etched configuration (**Design 6**) is fabricated on a low-cost FR-4. The system uses a dual-band operating frequency for testing, with -20 decibel reflection coefficients between 1.90 and 5.10 gigahertz and over 80% radiation efficiency; the highest realized gain is approximately 4.70 dBi and exhibits nearly omnidirectional radiation characteristics. Design number five was able to achieve superior performance in all performance categories when compared to four other designs, making it the best candidate to provide a low-profile and cost-effective antenna for compact multiband wireless and RF energy harvesting systems. The results of all tests conducted on the proposed antenna show similar performance characteristics between simulated and tested, with only minor differences attributable to manufacturing tolerances or the measurement being performed. Based on current information, the proposed antenna has proven to provide a viable solution for future low-cost compact and efficient multiband Wireless and RF Energy Harvesting Systems.*

Keywords: crescent-shaped antenna; microstrip patch antenna; etched radiator; multiband antenna; RF energy harvesting; antenna fabrication; measurement; VNA; return loss.

I. Introduction

The growing demand for compact, low-profile, multifunctional antennas that can operate over a wide range of frequencies is due to the rapid proliferation of modern wireless communication systems such as WLAN, Wi-Fi, IoT devices, biomedical sensors, and energy harvesting platforms [IX], [IV], [VI]. Microstrip patch antennas are very attractive for these types of applications because of their planar structure and ease of fabrication [IV], and a low-cost manufacturing process, as well as being compatible with integrated circuits[XXI]. However, conventional microstrip patch antennas are limited by their low gain, narrow bandwidth of operation, limited diversity of polarization, and the inherent nature of their design [X], [XVII].

Several studies have been conducted in this area to explore ways to overcome these limitations, including but not limited to the incorporation of slots, DGS structures, fractals, and modified radiator geometries [XII], [XI]. The geometric shaping of an antenna's radiating patch has been shown to be one of the more successful methods for improving an antenna's characteristics, such as bandwidth enhancement, multi-band (or dual band) operation, and dual-pol operation capability without increasing size significantly [XIV], [XXIV]. Crescent-shaped microstrip antennas are a good example of a shaped radiator that has multiple resonant modes due to the circularity of the edges and the curved shape, which in turn creates an extended surface current path [V], [XXIII]. The crescent-shaped microstrip antenna's asymmetrical shape makes it much easier to excite two separate current components (orthogonally), thus making this type of antenna ideally suited for dual-polarization and multi-band applications [XV], [XXIV]. The gradual curvature of the crescent-shaped microstrip radiator also provides for improved impedance matching and radiation efficiency in multiple frequency bands [XVIII], [XX].

Recent work investigating crescent and arc-shaped patch antennas for multiband and polarization-diverse applications has shown good improvement in their impedance bandwidth and radiation characteristics as compared to conventional rectangular and circular patch antennas [I], [XVII]. Nevertheless, few studies have been reported that focus on a single geometric [II] configuration while limiting investigation into how various geometrical modifications may impact the performance parameters of the antennas, such as return loss, VSWR, radiation efficiency, total efficiency, gain, and directivity [III], [XIX].

Taking these findings into consideration, this article describes the detailed study of six different types of crescent-shaped microstrip antennas created via various geometric shapes of the radiating elements. Each design was intended to enhance the performance of the antenna for particular aspects such as multiband operation, impedance matching to the impedances, polarization characteristics, and radiation efficiency. The antennas were simulated using CST Studio Suite, and their respective performance was analysed based on S parameters, VSWR, Radiation efficiency, total efficiency, gain, and directivity, as well as 3D radiation patterns. A detailed comparative analysis was made

to highlight how each geometric design impacted the performance characteristics of the antennas and to determine which design provided the best overall performance.

The following points summarise the main points of contribution:

Development of an optimised crescent-shaped microstrip antenna (MSA) that utilises various geometry-based methods to provide high radiation efficiency and appropriate impedance matching, enabling improved multiband operation for low-power wireless and RF energy harvesting applications.

Characterisation of six variations of an antenna structure developed from a baseline crescent radiator and modified through incremental channel refinement techniques, e.g., altering the width of the crescent, modifying the feed and ground arrangement, and implementing etched slots within the crescent structure.

Electrical performance of the developed antennas was characterised as exhibiting deep impedance matching characteristics, exhibiting reflection coefficients > -30dB at the dominant operating frequencies, and exhibiting VSWR values approaching unity, typical behaviour of optimally matched antennas, and confirming that efficient power transfer occurred via this type of structure

The ability of the crescent MSA to exhibit stable multiband characteristics throughout the desired frequency range would allow for the utilisation of multiple practical frequency bands in RF energy harvesting and wireless communication applications.

Despite the poor conductivity of FR4, the antenna demonstrated excellent radiation performance, with a radiation efficiency of > 90% and total efficiency > 92%. The total realised gain was as high as ~ 5 dBi.

At the final stage of design evolution, a novel etched crescent slot radiator configuration was implemented that improved overall surface current distribution and effective electrical length, producing enhanced MSAs without the necessity of increasing structural size or design complexity.

It was necessary to conduct an extensive evaluation of the full electromagnetic behaviour of the devised antenna designs through electromagnetic simulation in CST Studio Suite. The electromagnetic analysis included a complete evaluation of the reflection coefficient, VSWR, gain, directivity, efficiency, surface current distribution, and radiation patterns for the crescent MSAs.

Proposed compact, low fabrication cost, multiband capable high efficiency antenna structures are strong candidates for practical applications, including RF energy harvesting, IoT devices, low power wireless sensors, and compact communication systems.

The subsequent sections of this paper discuss the nature and implications of these points. Section 2 provides detailed information regarding the antenna configuration and additional analytical design equation references. Section 3 outlines the evolution of the antenna design through each respective configuration and analyses their respective characteristics. Section 4 presents a summary of both simulated and measured results, along with a comparative analysis. Finally, Section 5 offers conclusions regarding this research and presents areas of future research.

II. Antenna Structure and Design Methodology

A systematic design procedure is being used for the design of the crescent-shaped antenna as proposed by this project, with the start of the design proceeding with analytical calculations based on microstrip antenna theory and progressing through full-wave electromagnetic simulation and optimization to produce a fully optimized antenna utilizing these two techniques. This section describes the theoretical foundation and design principles for the antenna.

Antenna Geometry and Substrate Selection

The proposed antenna design will help modify the characteristics of surface current distribution, radiation characteristics, and impedance bandwidth to increase multipath capabilities. Microstrip antennas use geometry and size to determine their overall performance characteristics regarding how they will behave electromagnetically. Thus, a methodical, progressive approach is employed to keep control and enhance the performance of the antenna's ability to provide an efficient power transfer path between the source and the antenna it radiates from. It was made on an FR4 dielectric substrate with a compact footprint of 60×40×1.6 mm3 (length, width, and thickness), meaning it can easily fit into compact low-profile wireless devices or very small space-limited devices. The relative permittivity for the substrate (FR4) will be εr=4.4, and the loss tangent for the substrate (FR4) will be tan δ=0.02. To enhance impedance matching and radiation characteristics, a partial ground plane is provided on the bottom side of the FR4 substrate. A 50 Ω microstrip feed line provides excitation to the antenna to allow for maximal transfer of energy from the power source(s) to the antenna. Initially, when designing the antenna, a simple crescent-shaped microstrip patch was chosen as the baseline radiator that yields the fundamental resonances in the frequency of interest. Then, controlled geometric refinements were introduced into the design to improve the performance of the antenna by tweaking some of the dimensions of the crescent radiator, changes to the feed structure, and the partial ground plane utilized during manufacturing. Later in the design cycle, a crescent-emitted radiator structure was employed within the main radiator, thereby significantly altering the pathways of the surface currents, which resulted in increasing the effective electrical length. These changes allow the excitation of additional resonant modes, leading to improved impedance matching, multiband operation, and enhanced efficiency of the antenna's radiation.

Analytical Design Equations

The starting point for the design of the antennas was calculated in accordance with classical microstrip antenna theory and will be refined later by means of full-wave electromagnetic simulation.

Substrate Parameters

Substrate thickness: $h = 1.6$ mm
Relative permittivity (FR-4): $\varepsilon_r = 4.4$
Copper thickness: $t = 0.035$ mm
Effective Dielectric Constant

The effective dielectric constant accounts for the fringing fields and the inhomogeneous dielectric environment between the substrate and air:

$$\varepsilon_{\text{reff}} = \frac{\varepsilon_r + 1}{2} + \frac{\varepsilon_r - 1}{2}\left[1 + \frac{12h}{W_f}\right]^{-1/2}$$

where W_f is the microstrip feed-line width.

Microstrip Feed-Line Width

$$W_f = \frac{1.38\,c}{f_r\sqrt{\varepsilon_{\text{eff}}}}$$

where c is the speed of light in free space and f_r is the resonant frequency.

Effective Electrical Length of the Crescent Radiator

$$L_s = \frac{0.42\,c}{f_r\sqrt{\varepsilon_{\text{eff}}}}$$

Ground-Plane Dimensions

Length of the ground plane:

$$L_g = \frac{0.36\,c}{f_r\sqrt{\varepsilon_{\text{eff}}}}$$

Width of the ground plane:

$$W_g = \frac{8e^A}{e^{2A} - 2}, \qquad A = \frac{Z_0}{60}\sqrt{\frac{\varepsilon_r + 1}{2}} + \frac{\varepsilon_r - 1}{\varepsilon_r + 1}\left(0.23 + \frac{0.11}{\varepsilon_r}\right)$$

Resonant Frequency

$$f_r = 3 + \frac{2}{\sqrt{\varepsilon_{\text{eff}}}}\left[\frac{21}{L_s} + \frac{65}{W_g} + \frac{18}{L_g} - 3\right]$$

Using the above analytical equations as the basis for determining the initial dimensions of the antennas, a series of progressive geometrical optimizations has been conducted, resulting in six different antenna configurations; the geometries and feeding structures have been modified on a progressive basis from one configuration to the next.

III. Design Evolution and Configuration Details

A systematic study of the effect of shape change on antenna characteristics was conducted with the development of six series of antennas. Antennas were successively produced, with each of the designs being modified intentionally to create an improved design version. These design modifications include adding or changing elements (such as a crescent radiator), changing the feed mechanism, and using a different ground plane. These changes were made to increase the matching between antenna elements and improve multiband operation and radiation efficiency. The progressive design series can be seen in Fig 1, and a summary of each design's major features and parameters is in Table 1.

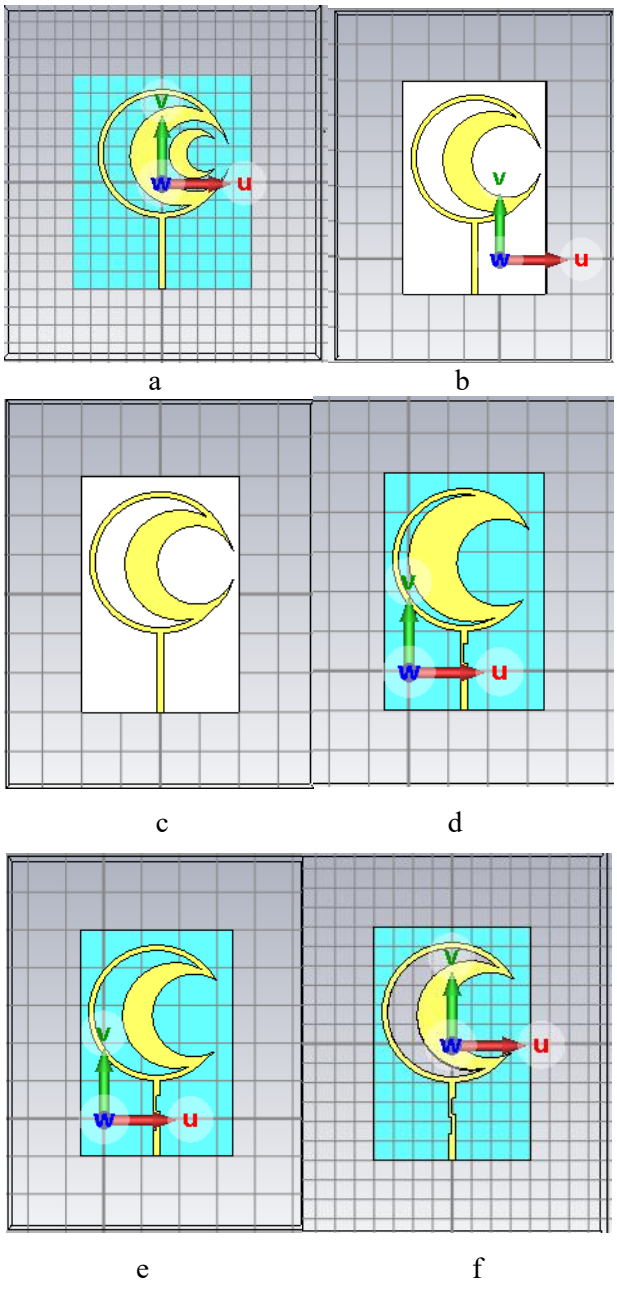

Fig. 1. (Crescent-Shaped Microstrip Antenna Design Evolution Steps) (a) Baseline crescent (Design 1) (b) Modified crescent (Design 2) (c) Enhanced current coupling (Design 3) (d) Multiband oriented crescent (Design 4) (e) Final optimized crescent (Design 5) (f) Etched crescent (Design 6)

Table 1. Geometrical parameters of the proposed antenna designs (units in mm).

Parameter	Design 1	Design 2	Design 3	Design 4	Design 5	Design 6
L_s	60	60	60	60	60	60
W_s	40	40	40	40	40	40
R_1	15	14	13.5	13	12.5	12
R_2	10	9	8.5	8	7.5	7
W_f	3.0	3.0	3.0	3.0	3.0	3.0
L_f	25	25	25	25	25	25
L_g	30	30	30	30	30	30
W_g	40	40	40	40	40	40

Note: Design 6 employs an etched crescent geometry within the same outer and inner radii to modify the surface current distribution.

Design 1: Baseline Crescent-Shaped Radiator

The base configuration for the developing crescent-shaped microstrip antenna is classified as design 1 and will be utilized as the benchmark to assess the impact of subsequent modifications due to geometric changes on the antenna structure. The antenna contains only one crescent-shaped radiating patch that is printed onto an FR 4 substrate using partial ground planes with a 50 Ω microstrip feed line connected to it. The data acquired from the simulated response for design 1 showed that the antenna: 1) had a resonance frequency value of approximately 4.25 GHz; 2) reflected the incoming signal at a very low level (-35.6 dB) and demonstrated an ideal voltage standing wave ratio (VSWR) value of 1.15. This indicates that there is an acceptable or ideal level of impedance matching over the main frequency band used by this antenna design. The maximum gain of the antenna is estimated to be 4.88 dBi, which corresponds to a high level of radiation efficiency (98.6%) and total efficiency (95.5%). However, this base design configuration has limited multiband properties and availability compared to the advanced configurations that can be implemented using multiple geometric modifications.

Design 2: Modified Crescent Geometry

Antenna design using controlled geometric alterations in design 2 was developed to improve both the coupling of surface currents from the antenna radiating element to its feed line and extend the overall effective electrical length of the crescent radiator. The antenna in design 2 also has a very good impedance match with an impedance value of -28.2 dB, resulting in a VSWR of 1.09, at a frequency of approximately 4.61 GHz, with a main resonance occurring at this frequency. Two additional resonant bands appear at approximately 1.8 GHz and 3.3 GHz, indicating the presence of multiband characteristics in this design. The maximum gain for an antenna of design #2 is 4.52 dBi, and the radiation efficiency is approximately 90% with an overall efficiency of approximately 61%.

Design 3: Enhanced Current Coupling Configuration

The additional geometrical design refinements of Design 3 would improve coupling to the surface current as well as prolongation of effective current paths. Ultimately, the simulated results for Design 3 reveal that there continues to be a clear multi-band response to Design 3, with the primary resonance being at 4.64 GHz (S11 = -32.38 dB) and the secondary resonating at roughly 2.1 GHz. Very close to the ideal range of 1.07, the VSWR is approximately 1.07. The radiation efficiency is around 93 percent; the total efficiency is estimated at 85 percent; and the peak gain is approximately 5.3 dBi.

Design 4: Multiband-Oriented Crescent Configuration

Design 4 improves upon the previous designs by modifying the geometry to enhance the coupling of the surface currents and allow the excitation of several resonant modes. The simulated results for Design 4 showed the resonant frequencies occurring at a frequency of approximately 1.78, 3.8, and 5.6GHz, respectively. The overall peak gain decreased to approximately 2.05dBi on the lower band from that of Design 3, but maintained a high radiation efficiency and reflected all RF energy with a minimum reflection coefficient of -20.9dB and a VSWR approaching 1.0.

Design 5: Final Optimized Crescent-Shaped Antenna

The design denoted as Design 5 is an optimized configuration with combined parameters selected from three components or systems: the crescent radiator, feed line, and ground plane. The Simulation results for Design 5 indicate that the antenna has a resonant frequency of 3.25GHz and that it has an S_{11} of -32.8 dB, VSWR >= 1, respectively, and that it provides maximum gain (5.09 dBi); directivity (5.34 dBi); radiating efficiency (94.3%), and total efficiency (93.6%). Consequently, this is the design with the strongest overall performance with respect to the measures of deep matching of input impedance, gain, efficiency, and consistency of performance in terms of pattern stability.

Design 6: Etched Crescent Configuration

Design 6 demonstrates a novel crescent etched radiator shaped like a crescent moon for the purpose of examining how slotted antennas behave differently from non-slotted antennas. The etched structure alters the distribution of currents on the surface of the antenna and facilitates the creation of different resonant modes. The jewelry model results of Design 6 show that the antenna has a strong resonance at 4.3 GHz with an S-parameter of -35.2 dB and a corresponding voltage standing wave ratio (VSWR) of approximately 1.3. The antenna has a maximum gain of 4.71 dBi and a radiation efficiency of 97.2%, while its overall efficiency is measured to be 92.9%. The etched crescent radiator redistributes the antenna currents across a larger effective area, leading to lower current concentrations, which leads to increased multiband excitations and increased radiating efficiency.

Performance Comparison of All Designs

The evaluation of the design evolution approach provided sufficient evidence to determine effective improvement within the six designs that were considered. The performance evaluation was completed on all six antenna configurations to

demonstrate how geometrical refinements from one design to the next can progressively enhance performance until a final, fully optimized design exists. Figure 2 shows the simulated reflection coefficient (S_{11}) responses for all six designs in the 1 – 7 GHz frequency range, indicating that as each design is refined, an improvement in matching the impedance response and resonant response occurs. Of all six configurations, Design 5 (the final optimized crescent-shaped antenna) was determined to have the best balance of performance in comparison to the other configurations. Design 5 develops a deep resonance at 3.25 GHz, which produces excellent impedance matching and an acceptable −10 dB bandwidth for practical implementation with wireless communications and RF Energy Harvesting applications. Design 6 (the etched crescent configuration) developed a wider bandwidth due to the etched design, as well as produced multiple resonant modes, but as a result, this design was focused more on multiband-type behaviors rather than optimizing a peak frequency. Design 5 provides the best balance between impedance and radiation and gain characteristics, which is the optimum design configuration in terms of overall electromagnetic performance, while also achieving the highest realized gain and best radiation efficiency of any of the designs evaluated thus far, confirming that the optimization process used was effective. The results of this performance evaluation confirmed that Design 5 is the most optimal antenna configuration considered in this paper, based on factors such as compactness, efficiency, and radiating capabilities.

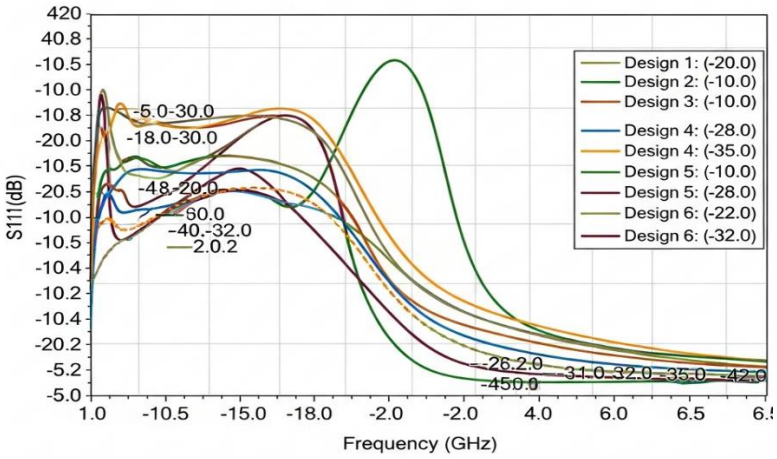

Fig. 1. Comparison of the simulated reflection coefficient (S_{11}) and peak gain for all antenna designs. **Design 5**, as the final optimized configuration, demonstrates the best overall performance in terms of impedance matching and gain.

Figure 3: The six proposed antenna configurations are compared graphically with regard to their peak performance gain characteristics, demonstrating an increase in gain performance with antenna geometry improvement from one design stage to another. Of all the designs tested, Design 5 was the last to be optimized, thus gaining the most from its final optimized design, resulting in the highest level of peak gain and therefore having the highest amount of radiation output due to the improved current distribution and geometry optimization. Design 4 has reduced as a comparison to both Design 5 and Design 6; therefore, Design 4 was used as an interim design between Design 3 and

Design 5 for demonstrating how the different designs affect overall performance and will provide evidence of how Design 5 has been validated for its superior performance when compared to both Design 4 and Design 6 when used in conjunction with the proposed antenna design configurations.

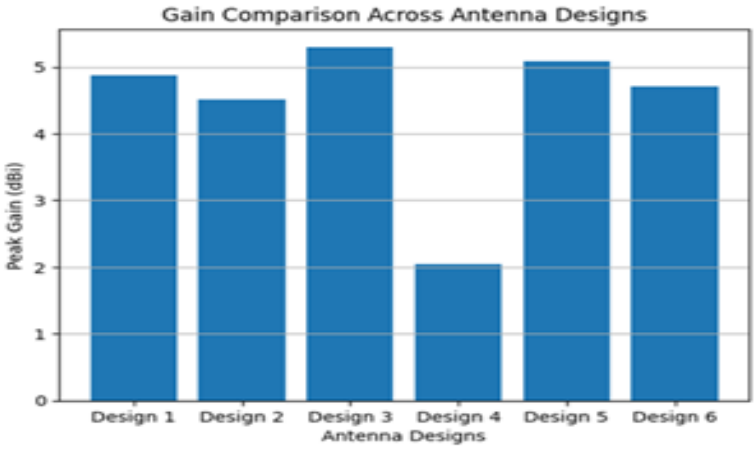

Fig.3. It represents the gain comparison among the antennas

Parametric Analysis

The results of a detailed parametric study helped to identify how changes in geometry affect how the antenna performs, which was used to optimize the design. The results also provided insight into which of the design dimensions are critical to the final performance of the antenna. The plot in Figure 4 shows how the change in crescent radius from 15 mm to 7 mm caused the change in the frequency at which the antenna operates, or resonates, from 3.8 GHz to 4.3 GHz (or back down to the frequency of 3.8 GHz). The crescent radius has a direct effect on the antenna operating frequency.

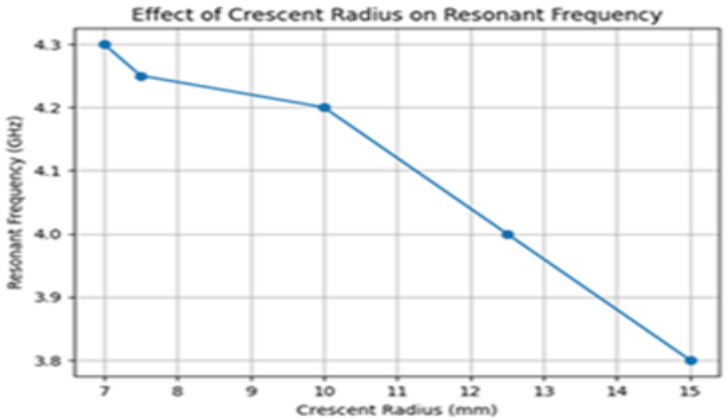

Fig.4. It illustrates the effect of crescent radius variation on resonant frequency. As the radius decreases from 15 mm to 7 mm, the resonant frequency shifts from 3.8 GHz to 4.3 GHz.

IV. Antenna Fabrication and Experimental Measurement

This is a key milestone in the journey from simulated design to actual product (antenna). In this section, the details are provided regarding both the fabrication and tests of the proposed etched crescent antenna.

Fabrication Setup

We have manufactured Design5, our etched crescent antenna, utilizing an LPKF laser etching system (e.g., Figure 5), allowing us to achieve very accurate copper patterns on an FR-4 board. The FR-4 board we used was a standard thickness of 1.6 mm (0.063 inches) and had a dielectric constant (ε_r) of 4.4. The antenna also had a copper conductor thickness of 35 μm (0.035 mm), and we employed a partial ground plane on the bottom side of the antenna to improve its impedance matching and increase its bandwidth.

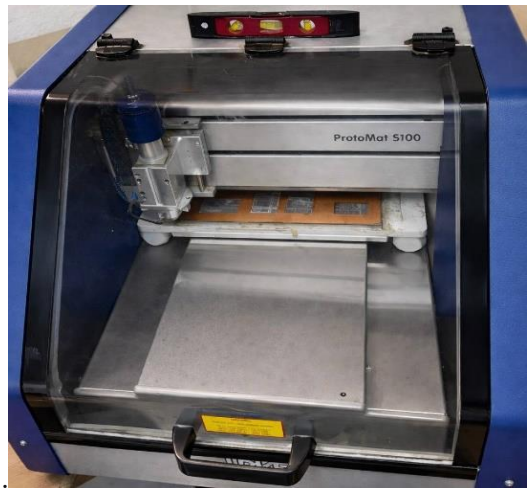

Fig. 5. LPKF laser etching machine used for antenna fabrication (warning labels indicate laser safety precautions).

Fabrication Steps

• Substrate Preparation: Using alcohol to clean and properly prepare the FR-4 substrate, then drying well to avoid dust and contaminants.

• Laser Etching: The LPKF laser system was used to etch out the crescent-shaped radiator, microstrip feed line, and partial ground plane based on the final and validated design dimensions.

• Cutting: The completed antenna was finally cut to 60 × 40 mm².

• SMA Connector Attachment: The microstrip feed line was soldered to the ground plane to attach a 50-ohm SMA connector for testing purposes.

Fabricated Prototype

This is an example of a fabricated antenna prototype (shown in Figure 6) with the front view (showing the engraved crescent radiator) and back view (showing the partial

ground plane). The fabricated structure reflects excellent agreement with the design optimization, and this confirms that it's possible to manufacture, have dimensional accuracy, and structural integrity of the proposed antenna.

Fig. 6. Fabricated crescent-shaped microstrip antenna prototypes showing the etched radiator and partial ground plane on an FR-4 substrate.

V. Measurement Setup and Experimental Validation

To confirm that our simulation results for this design are valid, we will conduct accurate experiments to validate our findings. In this section, we will provide details about our measurement setup and equipment used to evaluate the prototype that was manufactured.

Vector Network Analyzer (VNA) Measurement

The parameter S_11, which represents the reflection coefficient, was obtained using an Anritsu Vector Star MS4647B VNA (see Figure 7). The process used to conduct these measurements is detailed in the flowchart presented in Figure 9, which allowed for systematic and repeatable measurement acquisition.

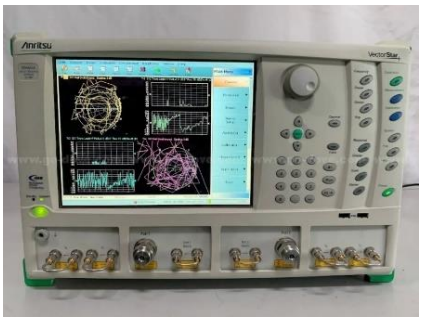

Fig. 7. Anritsu VectorStar VNA used for S_11 measurement.

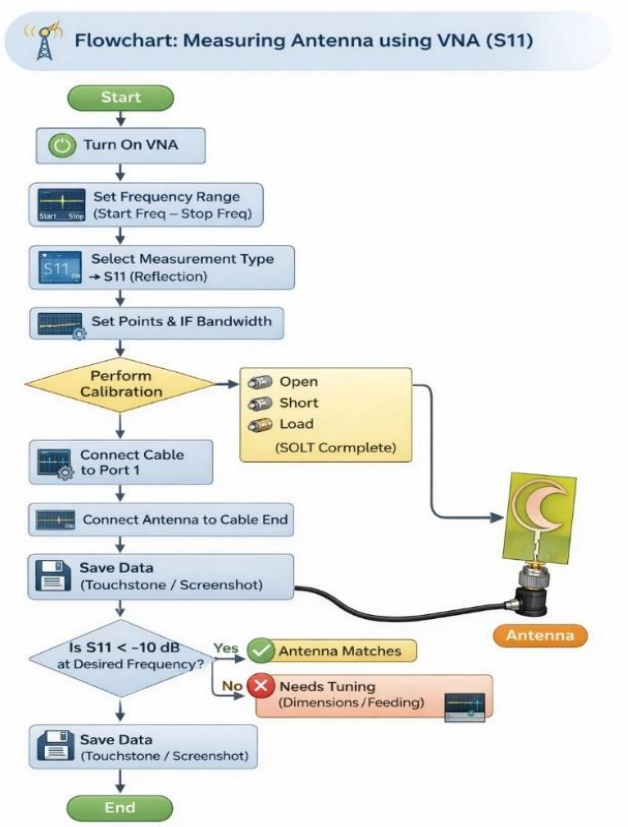

Fig. 8. Flowchart of antenna measurement process using VNA.

Measurement Steps:

The measurement setup includes an Anritsu VectorStar MS4647B VNA, calibrated using the SOLT method from 1–7 GHz. The antenna was measured in an anechoic chamber to minimize environmental reflections, as shown in fig-9:

1. The Vector Network Analyzer (VNA) was calibrated by using a Short, Open, Load, and Through (SOLT) Calibration Kit and connected to the RF Cable, and the full 2-port calibration process was completed via SOLT calibration.
2. The total frequency range was between 1.0 GHz and 7.0 GHz in order to cover all resonant areas of the antenna.
3. An antenna was connected to Port 1 on the VNA using an RF cable, as shown in Fig. 9.
4. The S_{11} (Return Loss) data obtained from testing were compared between the actual return loss measurements from the VNA and the theoretical results obtained through simulation.

Fig. 9. Measurement setup: antenna connected to VNA via RF cable

V.i. Simulated vs. Measured Return Loss

Figure 10 presents the comparison between the simulated (predicted) and the measured (actual) return loss (S11) values of Design 6 within the frequency range of 1 to 7 GHz. The comparison of both sets of data provides valuable insight regarding the correlation of the theoretical predictions to the actual performance of the etched crescent design. Overall, the measured return loss data follow a pattern similar to the simulated return loss responses, validating the effectiveness of the manufactured etched crescent design. Some minor differences are noted between the depth of the resonances and a slight frequency shift, which can primarily be attributed to fabrication tolerances, connector losses, and measurement errors. Even with these slight discrepancies, Design 6 has maintained a sufficient level of impedance matching with the return loss values of less than -10 dB at the primary operating bands. Based on these results, it can be concluded that Design 6 exhibits good multiband performance; however, the overall frequency stability and resonance depths are not quite as consistent compared to the optimized final design.

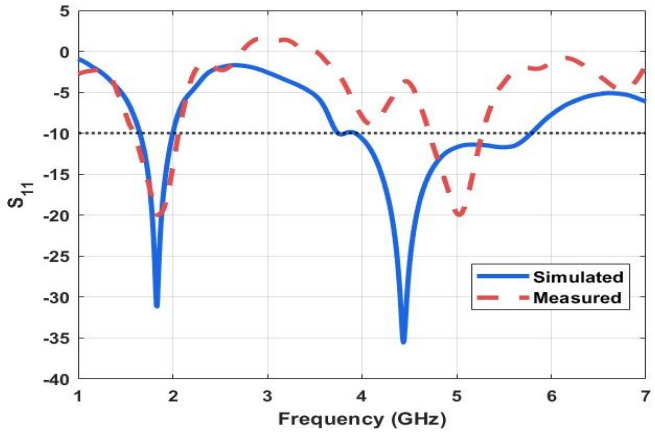

Fig. 10. Comparison of simulated and measured return loss (S_11) for Design 6.

The graph depicts the return loss (S11) comparison of Design 5, the final optimized antenna configuration, between measured results and simulated return losses. The simulated and measured results show strong agreement, especially at the major resonant frequencies. The measured results track nearly identically to the simulated results, showing a deep resonance and stable impedance matching across the frequencies of interest. There are minor variations in terms of resonance depth and frequency, but they are within acceptable limits and do not impact the antenna's overall performance. Design 5 produces a more stable resonance response, a deeper return loss, and a better agreement between measurement and simulation than all other designs, further verifying its superior impedance matching characteristics. The results from Design 5 support its use as the superior and end design for production use in practical wireless and RF energy harvesting applications.

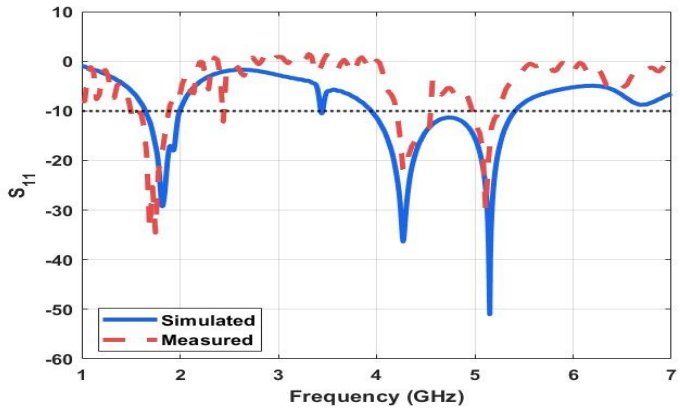

Fig. 11. Comparison of simulated and measured return loss (S_11) for Design 5

VI. Performance Comparison and Discussion

Table 2 shows the performance of our crescent antenna designs (Designs 5 and 6) compared to several new multiband antennas that were previously reported. Although the antenna is compact (60 × 40 mm²), it has an excellent impedance match

(less than −10 dB at the bands), excellent radiation efficiencies (>93%), and provides good multiband and dual-band operation. Therefore, it is suitable for use with RF energy harvesting and as a compact antenna for wireless devices, as seen in Fig. 12.

Table 2: It provides a detailed comparison with the literature:

Reference	Size (mm²)	Operating Bands (GHz)	Peak Gain (dBi)	Radiation Efficiency (%)	Design Complexity
[XXVI]	100×60	2.17-2.72, 3.34-3.66	3.75	~85	Moderate
[VIII]	30×65	2.375-2.525, 3.075-3.80	5.20	~88	Moderate
[VII]	40×45	2.02-2.14, 4.26-4.28	4.13	~82	Complex
This Work	60×40	1.9, 4.2, 5.2	5.1	93	Low
		1.5-5.0	4.71	>80	Low

Figure 12 provides a curve-based comparison of the normalized results for each metric, which produces a three-dimensional view of how this work also compares to other current state-of-the-art antennas in regard to different categories. The graphical representations show that the proposed new antenna provides an excellent overall performance index.

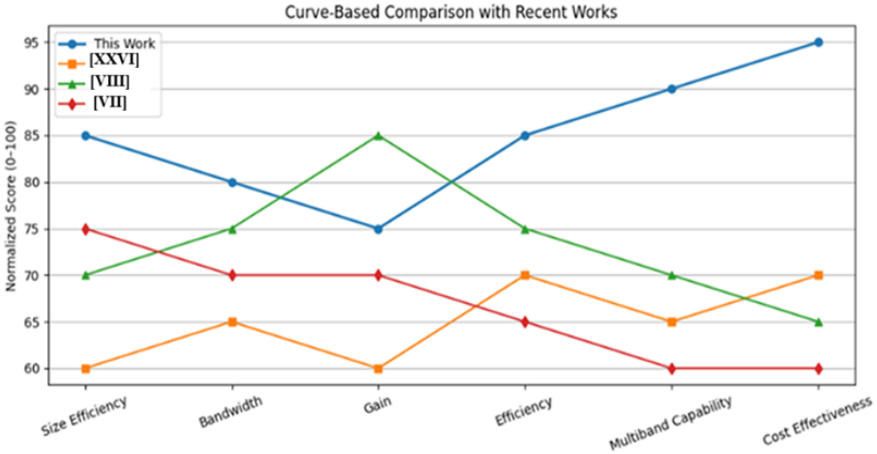

Fig. 12. It shows a radar chart comparing key metrics

The performance metrics demonstrate that the etched crescent geometry reduces the loss caused by the current and dielectric materials by redistributing the surface current and minimizing the localized current crowding. As indicated by the results, the proposed design has superior performance to other compact antenna designs that use similar substrate materials.

VII. Conclusion and Future Work

This study details thorough research on a crescent-shaped etched microstrip patch antenna, suited for small multi-band wireless applications, RF energy harvesting capabilities, and has undergone a structured development process of six different design variations, showing that sequential evolution of geometry significantly enhances

the performance. The final optimized design 5 achieved the best multiband functionality, with improved matching of impedance ($S_{11} < -10$ dB across all bands) as well as high efficiency (>80%) and steady characteristics of radiation. The experimental verification and fabrication aligned well with expected results, given minor discrepancies due to tolerances in fabrication and set-up challenges. Additionally, it demonstrates that antennas can support multiple wireless communication bands for WLAN, Wi-Fi, and IoT applications while maintaining a small physical footprint of 60 × 40 × 1.6 mm on a low-cost substrate (FR-4). The contributions to this effort include: (1) showing the effectiveness of the etched crescent-shaped antenna for increasing multiband performance without enlarging the size of the antenna; (2) providing a method of systematic optimization of multiple performance variables; (3) providing verified experimental data demonstrating that the radiation efficiency (>80%) can be attained using low-cost FR-4 substrate; and (4) demonstrating competitive performance with the latest state-of-the-art designs in terms of trade-offs between size, bandwidth, and efficiency. The antenna design has many practical benefits for wireless systems today, especially in applications where compactness, multiband capability, and cost-effective solutions are essential. The etched crescent design is behind much of the future's work in miniaturization and enhancement of antenna performance, with application potential to many other frequency ranges and related use cases in the future.

Conflict of Interest:

The authors declare that there was no relevant conflict of interest regarding this paper.

References

I. Aafizaa, K., Uma Haimavathi, K., & Saravanan, S. (2026). Recent Innovations in Microstrip Patch Antennas: Biomedical Uses and Wireless Integration. Biomedical Materials & Devices, 4(1), 326-341.

II. Abbas, R. A., & Kadhum, M. H. (2024). A Review of Energy Harvesting Techniques for Self-Powered IoT Devices. Wasit Journal of Engineering Sciences, 12(4), 133-145.

III. Ahmad, I., Tan, W., Ali, Q., & Sun, H. (2022). Latest performance improvement strategies and techniques used in 5G antenna designing technology, a comprehensive study. Micromachines, 13(5), 717.

IV. Almawlawe, M. D. H., Al-Araji, Z., & Saitkulov, V. (2025). Impact of Substrate Dielectric Constant on Performance of 2.4 GHz Microstrip Patch Antenna Array. Wasit Journal of Engineering Sciences, 13(1), 22-38.

V. Aras, U., Delwar, T. S., Durgaprasadarao, P., Sundar, P. S., Ahammad, S. H., Eid, M. M., Lee, Y., Zaki Rashed, A. N., & Ryu, J.-Y. (2024). Dual features, compact dimensions and X-band applications for the design and fabrication of annular circular ring-based crescent-moon-shaped microstrip patch antenna. Micromachines, 15(7), 809.

VI. Arnaoutoglou, D. G., Empliouk, T. M., Kaifas, T. N., Chryssomallis, M. T., & Kyriacou, G. (2024). A review of multifunctional antenna designs for internet of things. Electronics, 13(16), 3200.

VII. Babu, G. H., Srinivas, M., Gnanaprakasam, C., Prabu, R. T., Devi, M. R., Ahammad, S. H., Hossain, M. A., & Rashed, A. N. Z. (2023). Meander line base asymmetric co-planar wave guide (CPW) feed tri-mode antenna for Wi-Max, North American Public Safety and satellite applications. Plasmonics, 18(3), 1007-1018.

VIII. Dadhich, A., Samdani, P., Deegwal, J., & Sharma, M. (2019). Design and investigations of multiband microstrip patch antenna for wireless applications. In Ambient Communications and Computer Systems: RACCCS-2018 (pp. 37-45). Springer.

IX. Gatea, Q. M., & Ali, F. M. (2025). Design and Implementation of High-Gain Wide-Bandwidth Patch Antenna Array 5G Base Stations. Wasit Journal of Engineering Sciences, 13(3), 51-61.

X. Ghorbani, A., Ansarizadeh, M., & Abd-Alhameed, R. (2009). Bandwidth limitations on linearly polarized microstrip antennas. IEEE Transactions on Antennas and Propagation, 58(2), 250-257.

XI. Guha, D., Kumar, C., & Biswas, S. (2022). Defected ground structure (DGS) based antennas: design physics, engineering, and applications. John Wiley & Sons.

XII. Husien, N. Q. A., & Al-khazaali, H. F. K. (2024). Design of Microstrip Antenna Array for Autonomous Vehicles. Wasit Journal of Engineering Sciences, 12(4), 103-112.

XIII. Ibrahim, H. H., Singh, M. J., Al-Bawri, S. S., Ibrahim, S. K., Islam, M. T., Alzamil, A., & Islam, M. S. (2022). Radio frequency energy harvesting technologies: A comprehensive review on designing, methodologies, and potential applications. Sensors, 22(11), 4144.

XIV. Isa, S. R., Jusoh, M., Sabapathy, T., Nebhen, J., Kamarudin, M. R., Osman, M. N., Abbasi, Q. H., Rahim, H. A., & Yasin, M. N. M. (2022). Reconfigurable Pattern Patch Antenna for Mid-Band 5G: A Review. Computers, Materials & Continua, 70(2).

XV. Kaim, V., Singh, N., Kanaujia, B. K., Matekovits, L., Esselle, K. P., & Rambabu, K. (2022). Multi-channel implantable cubic rectenna MIMO system with CP diversity in orthogonal space for enhanced wireless power transfer in biotelemetry. IEEE Transactions on Antennas and Propagation, 71(1), 200-214.

XVI. Khandelwal, M. K., Kanaujia, B. K., & Kumar, S. (2017). Defected ground structure: fundamentals, analysis, and applications in modern wireless trends. International Journal of antennas and Propagation, 2017(1), 2018527.

XVII. Mishra, B., Verma, R. K., & Singh, R. K. (2022). A review on microstrip patch antenna parameters of different geometry and bandwidth enhancement techniques. International Journal of Microwave and Wireless Technologies, 14(5), 652-673.

XVIII. Quan, L., Zhong, X., Liu, X., Gong, X., & Johnson, P. A. (2014). Effective impedance boundary optimization and its contribution to dipole radiation and radiation pattern control. Nature communications, 5(1), 3188.

XIX. Räsänen, M. (2023). Design and analysis of a high-gain and wide-band phased-array antenna for V-band.

XX. Ren, Y., Luo, W., He, Z., Qin, N., Meng, Q., Qiu, M., Li, J., Yang, H., Xu, L., & Li, Y. (2025). Development and performance study of a radiation-enhanced heat pipe radiator for cooling high-power IGBT modules. Applied Thermal Engineering, 262, 125307.

XXI. Sabban, A. (2022). Wearable circular polarized antennas for health care, 5G, energy harvesting, and IoT systems. Electronics, 11(3), 427.

XXII. Sabban, A. (2024). Green wearable sensors and antennas for bio-medicine, green internet of things, energy harvesting, and communication systems. Sensors, 24(17), 5459.

XXIII. Sharma, V. (2020). Microstrip antenna-inception, progress and current-state of the art review. Recent Advances in Electrical & Electronic Engineering (Formerly Recent Patents on Electrical & Electronic Engineering), 13(6), 769-794.

XXIV. Suganya, E., Pushpa, T. A. J. M., & Prabhu, T. (2024). Advancements in patch antenna design for Sub-6 GHz 5G smartphone application: a comprehensive review. Wireless personal communications, 137(4), 2217-2252.

XXV. Suryapaga, V., & Khairnar, V. V. (2024). Review on multifunctional pattern and polarization reconfigurable antennas. IEEE Access, 12, 90218-90251.

XXVI. Zainud-Deen, S. H., El-Shalaby, N. A., Malhat, H. A., & Gaber, S. M. (2019). Reconfigurable multi-turns planar plasma helical antenna. Plasmonics, 14(6), 1831-1837.